第33卷 第1期 焊 接 学 报 Vol. 33 No. 1
2012年1月 TRANSACTIONS OF THE CHINA WELDING INSTITUTION January 2012

超声对不同铝合金搅拌摩擦焊接头性能的影响

马慧坤， 贺地求， 刘金书
(中南大学 机电工程学院，长沙 410083)

马慧坤

摘 要：利用自行研制的超声搅拌摩擦焊机分别对2219，7A52，LF21铝合金进行了常规搅拌摩擦焊和超声搅拌摩擦焊两种不同焊接的试验，并对常规搅拌摩擦焊与超声搅拌摩擦焊焊缝的微观组织、拉伸断口形貌进行了对比分析. 结果表明，超声搅拌摩擦焊与常规搅拌摩擦焊相比热影响区几乎消失；超声搅拌摩擦焊焊缝焊核区组织比常规搅拌摩擦焊焊核区组织晶粒更加细小；断口扫描电镜图显示母材断口韧窝具有非等轴状待征，韧窝边上撕裂棱明显表明为韧性断裂；超声搅拌摩擦焊断口韧窝撕裂棱不明显；超声搅拌摩擦焊比常规搅拌摩擦焊的平均抗拉强度有所提高，但断后伸长率有所降低.

关键词：搅拌摩擦焊； 超声； 性能
中图分类号：TG115.28 **文献标识码**：A **文章编号**：0253－360X(2012)01－0006－03

0 序 言

搅拌摩擦焊接(friction stir welding，FSW)是由英国焊接研究所(TWI)于20世纪90年代初发明的一种新型固态连接技术. 随着航天、军工和汽车等行业对熔焊性差的高强铝合金等特殊材料的需求量不断增加，推动了搅拌摩擦焊接技术的发展，并成为21世纪国内外研究的热点. 它不仅具有高质量、低成本、低变形，易于自动化等特点，而且不需要填充材料和保护气、能耗低，对环境无污染. 同时，搅拌摩擦焊接后结构的残余应力或变形也较熔化焊小得多，是一种理想的绿色连接技术[1,2]. 对于热塑性较好的铝合金，FSW可得到较高强度的焊缝，适用于多种铝合金的焊接[3－5]. 它是通过高速旋转的搅拌头与被焊材料间剧烈的热机联合作用而实现的固相连接. 影响搅拌摩擦焊接头质量的主要因素是焊接过程中搅拌摩擦的发热量和待焊材料在搅拌头作用下的塑性流动过程. 它与焊接工艺参数有关. 目前提高接头力学性能的主要方式是改变搅拌头的形状、焊接速度、搅拌头旋转频率、焊接倾角和轴肩压入深度等工艺参数. 为了进一步增加搅拌针周围金属的流动性，提高焊缝力学性能，文中利用超声搅拌摩擦焊对三种不同型号的铝合金进行了焊接试验，并对常规搅拌摩擦焊与超声搅拌摩擦焊焊缝的力学性能、微观组织、拉伸断口形貌进行了分析. 对比验证了不同系列的铝合金对超声的敏感性和超声搅拌摩擦焊对铝合金焊接的可行性.

收稿日期：2011－03－02
基金项目：国家自然科学基金资助项目(500675228)

1 试验方法

试验利用中南大学自行研制的超声搅拌摩擦焊机分别对2219，7A52，LF21铝合金进行了常规搅拌摩擦焊和超声搅拌摩擦焊两种不同的焊接试验. 通过大量试验选取常规搅拌摩擦焊接头性能最适合的工艺参数作为超声搅拌摩擦焊的工艺参数，使得两种焊接试验结果在相同参数下具有横向可比性. 焊接工艺参数见表1.

表1 焊接工艺参数
Table 1 Welding parameters

铝合金型号	焊接速度 v/(mm·min^{-1})	旋转频率 n/(r·s^{-1})
2219	106.8	16.67
7A52	40	24.17
LF21	71.2	33.33

焊接完成后，用线切割机横向切割取样取焊缝的横截面制作金相试样，对断面用碳化矽砂纸(400号～2000号)进行粗磨和精磨，然后在抛光机上加抛光液用绒布抛光到镜面水平，最后再经过适当的化学腐蚀处理得到试样. 腐蚀时间短晶界不明显，在显微镜下观测不到晶界. 腐蚀时间过长则出现很深的腐蚀坑，形成过腐蚀. 将腐蚀好的试样表面清洗擦干，在POLYVAR2MET光学显微镜上观察其金相组

织. 在 CSS-44100 电子拉伸机上对焊接试样进行拉伸试验,用 JEOL JSM-6360LV 型扫描电镜仪观察其断口形貌.

2　试验结果及分析

2.1　接头力学性能分析

2.1.1　2219 接头力学性能试验结果

从拉伸试验数据分析可知,常规搅拌摩擦焊的抗拉强度为 336 MPa,达到母材的 73.9%,平均断后伸长率约为 2%,超声搅拌摩擦焊试样的抗拉强度为 352 MPa,达到母材的 77.5%,平均断后伸长率约为 1.8%,初步得出超声搅拌摩擦焊试样的抗拉强度相对常规搅拌摩擦焊的抗拉强度提高 16 MPa,为母材 3.6%,但是平均断后伸长率有所降低.

2.1.2　7A52 接头试样力学性能试验结果

7A52 常规搅拌摩擦焊接头的抗拉强度为 376 MPa,达到母材的 75.7%,平均断后伸长率约为 2.7%,超声搅拌摩擦焊试样的抗拉强度为 380 MPa,达到母材的 76.7%,平均断后伸长率约为 1.6%,抗拉强度提高 5 MPa,平均断后伸长率低于常规搅拌摩擦焊.

2.1.3　LF21 接头力学性能试验结果

LF21 常规搅拌摩擦焊的抗拉强度为 116 MPa,达到母材的 89.1%,平均断后伸长率约为 9.3%,超声搅拌摩擦焊试样的抗拉强度为 128 MPa,达到母材的 98.1%,平均断后伸长率约为 7.3%,超声搅拌摩擦焊试样的抗拉强度相对常规搅拌摩擦焊的抗拉强度提高 12 MPa,达 10.1%,但是平均断后伸长率有所降低.

试验表明,超声搅拌摩擦焊的平均抗拉强度都比常规搅拌摩擦焊的平均抗拉强度有所提高,但平均断后伸长率均有所降低.

2.2　焊缝微观组织

将制作好的试样在 POLYVAR2MET 光学显微镜上分别观察常规搅拌摩擦焊(图 1)和超声搅拌摩擦焊金相组织(图 2).

由图 1,图 2 可以看出两种焊核区晶粒非常细小,是明显的再结晶等轴晶粒,常规搅拌摩擦焊焊核区晶粒大小在 4 μm 左右,但是加入了超声作用的焊缝焊核区组织比未加入超声的焊核区组织晶粒明显更加细小,枝晶不明显,成为更加细小等轴晶,而且分布较为均匀,晶粒大小在 1 μm 左右. 这一现象说明超声振动的能量注入到焊缝,对焊核区,特别是焊核区的底层金属组织有明显的晶粒细化和组织均匀化的积极效果.

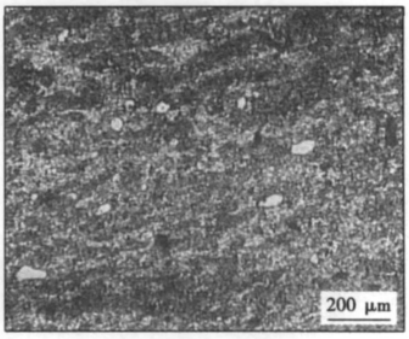

图 1　常规搅拌摩擦焊焊核区

Fig. 1　Weld nugget zone of FSW

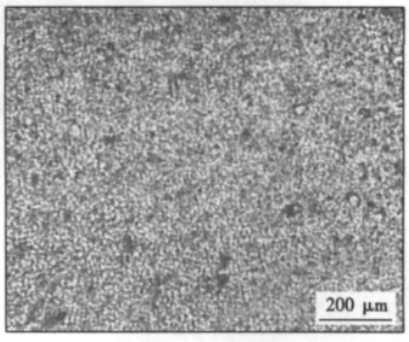

图 2　超声搅拌摩擦焊焊核区

Fig. 2　Weld nugget zone of ultrasonic friction stir welding

超声搅拌摩擦焊(图 3)与常规搅拌摩擦焊的热影响区(图 4)相比几乎消失,组织分布较为均匀,表明超声振动的能量成功地注入到焊缝. 这是机械作用效应和体积效应所致,即超声振动使焊缝的金属微粒获得巨大的能量,产生高频振动,金属微粒的热运动加剧,使金属组织有明显的晶粒细化和组织均匀化的积极效果,从而改善焊缝效果.

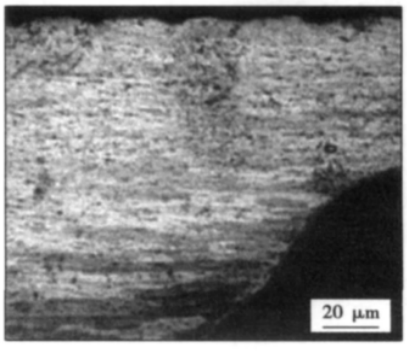

图 3　超声搅拌摩擦焊热影响区和热力影响区

Fig. 3　TMAZ and HAZ of ultrasonic friction stir welding

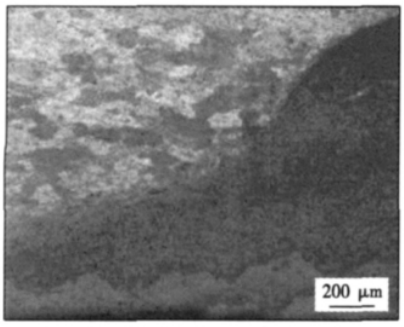

图 4 常规搅拌摩擦焊热影响区和热力影响区
Fig. 4 TMAZ and HAZ of FSW

2.3 接头拉伸断口形貌分析

采用 JEOL JSM-6360LV 型扫描电镜仪，将断口放大到 20 μm 观测断口处的撕裂状况. 图 5 为母材断口电镜扫描形貌，图 6 为超声搅拌摩擦焊断口电镜扫描形貌. 两者相比，图 5 母材的撕裂棱更为明显，图 6 超声搅拌摩擦焊断口电镜扫描几乎看不到撕裂棱.

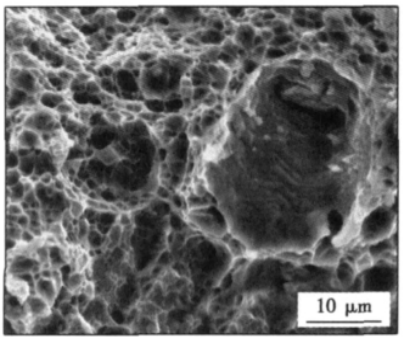

图 5 母材断口电镜扫描
Fig. 5 SEM of base material

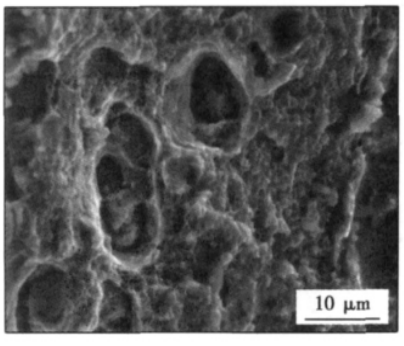

图 6 超声搅拌摩擦焊断口电镜扫描
Fig. 6 SEM of ultrasonic friction stir welding

图 5 中，母材的断口分布有直径约为 8 ~ 20 μm 大韧窝，这是因为所焊轧制板材的晶粒在经过轧制后，发生了较大的变形，使其断口韧窝具有非等轴状特征. 窝内部还存在一些平均直径 2 μm 的小韧窝和撕裂棱，显示断裂形式为韧性断裂.

超声搅拌摩擦焊的断口表面以及大韧窝内部的小韧窝不明显，也没有比较清晰的撕裂棱，见图 6. 从两者断口电镜扫描形貌可以得出超声搅拌摩擦焊韧性与母材相比较差. 这种微观组织使得超声搅拌摩擦焊试样表现为力学性能断后伸长率降低.

3 结 论

(1) 常规搅拌摩擦焊和超声搅拌摩擦焊两种焊接方法的焊缝外观成形良好，表面平整，无严重的飞边，匙孔内光滑，无明显空洞缺陷.

(2) 超声搅拌摩擦焊的平均抗拉强度都比常规搅拌摩擦焊的的平均抗拉强度有所提高，但平均断后伸长率均有所降低.

(3) 超声搅拌摩擦焊焊缝焊核区组织比常规搅拌摩擦焊焊核区组织晶粒明显更加细小，枝晶不明显，成为更加细小等轴晶，分布较为均匀.

(4) 超声振动使焊缝的金属微粒获得巨大的能量，产生高频振动，金属微粒的热运动加剧，超声搅拌摩擦焊与常规搅拌摩擦焊相比热影响区几乎消失.

参考文献：

[1] Joelj D. The friction stir welding advantage [J]. Welding Journal, 2001, 80(5): 30 - 34.

[2] Mishra R S, Ma Z Y. Friction stir welding and processing [J]. Materials Science and Engineering R, 2005, 50(2): 1 - 78.

[3] Hanadi S G. Friction stir weld evolution of dynamically recrystallized AA 2095 weldments [J]. Scripta Materialia, 2003(49): 1103 - 1110.

[4] Peel M, Steuwer A, Preuss M, *et al*. Microstructure, mechanical properties and residual stress as a function of welding speed in aluminium AA 5083 friction stir welds [J]. Acta Materialia, 2003(51): 4791 - 4801.

[5] Cabibbo M, Mcqueen H J, Evangelista E, *et al*. Microstructure and mechanical property studies of AA 6056 friction stir welded plate [J]. Materials Science and Engineering A, 2007(460 - 461): 86 - 94.

作者简介： 马慧坤，男，1977 年出生，博士研究生. 主要从事搅拌摩擦焊工艺及机理方面的研究. 发表论文 5 篇. Email: liujsmhk@126.com

通讯作者： 贺地求，男，教授. Email: hdqzzp@163.com

MAIN TOPICS, ABSTRACTS & KEY WORDS

Design and implementation of a power control system for electron beam welder HE Shaojia, LI Jianling, MO Jinhai, LI Haibiao (School of Mechanical & Electrical Engineering, Guilin University of Electronic Technology, Guilin 541004, China). pp 1 – 5, 12

Abstract: Stability of output voltage of high-voltage accelerating stabilized power supply for electron beam welder (EBW) is a prerequisite to ensure the electron beam welding quality. The common power supplies have the disadvantages of circuit complexity and bulkiness. A novel control system of high-voltage accelerating stabilized power supply for EBW was designed. Its main circuit is based on pulse-width modulation (PWM) buck-boost converter topology. Compared with common EBW power supplies, this new power supply requires a much lower voltage grade transformer because of the converter's effect for rising voltage, so its volume is smaller and the circuit is simpler. The system main circuit characteristics and its working process were analyzed. The system circuit's small-signal mathematical model was created, and lag-lead correction compensation control was employed in the system to achieve static and dynamic performance requirements. The results displayed that this unit had the characteristics of fast response, high reliability, high control precision and anti-interference capability.

Key words: electron beam welder; buck-boost converter; simulation

Effects of ultrasonic on properties of joints welded by friction stir welding process MA Huikun, HE Diqiu, LIU Jinshu (College of Mechanical and Electrical Engineering, Central South University, Changsha 410083, China). pp 6 – 8

Abstract: In this paper, joints of 2219, 7A52 and LF21 aluminum alloy were obtained by using a self-made ultrasonic friction stir welding machine. The microstructures and fractography of these joints were studied. The results show that the thermal mechanically affected zone (TMAZ) of ultrasonic friction stir welding is almost disappearing; The grains of weld nugget zone (WNZ) by ultrasonic friction stir welding are much finer than the ones obtained by conventional friction stir welding; The tensile fracture of base material appears to be mixed fracture with dimple and tear ridges. The tensile fracture of ultrasonic friction stir welding appears to be a dimple pattern. Although the tensile strength of joints obtained by ultrasonic friction stir welding are higher than the ones obtained by conventional friction stir welding, the elongation of the joints fellow on opposite tendency.

Key words: friction stir welding; ultrasonic; property

Effects of welding materials on hot crack of spray formed 7475 Aluminum alloy in TIG welding joint YAN Keng, YE Youli, WANG Xiling (Provincial Key Lab of Advanced Welding Technology, Jiangsu University of Science and Technology, Zhenjiang 212003, China). pp 9 – 12

Abstract: In this paper, the spry formed 7475 aluminium alloy was welded by TIG welding process with the welding consumable 4043, 5356 and 7055 respectively. The susceptibilities of hot cracking, as well as the mechanical properties, microstructures, the morphologies and the phase compositions of joints were studied in all three kinds of welding consumables. The results showed that susceptibility of hot cracking of welding material 5356 was closely related to the heat input. In condition of high heat input, Cu and Zn in parental material diffuse to weld and form low melting point eutectic phased α-Al, $Al_{0.403}Zn_{0.597}$ and $Al_7Cu_3Mg_6$ at fusion area with Mg from weld. And then they segregate at inter-granular and inter-dendrite. Therefore, penetrated hot cracks appeared in the fusion area under the action of welding stress. No crack appeared in condition of low heat input but the tensile strength of welded joint was only 184MPa. However, hot cracking susceptibilities of welding consumables 4043 and 7055 are relatively lower.

Key words: spray formed aluminum alloy; TIG welding; hot crack

A analysis method of seam tracking accuracy based on wheeled robot HONG Bo, ZHANG Qilin, LI Xiangwen, YIN Li (School of Mechanical Engineering, Xiangtan University, Xiangtan 411105, China). pp 13 – 16

Abstract: Based on the research of the wheeled robot seam tracking accuracy in 4 degrees of freedom, a new characterization assessment of seam tracking accuracy method was proposed, and 5-parameter model under D-H coordinate system in seam bias was built up as well. By this model, the main error sources affecting the accuracy of seam tracking is theoretically analyzed. Through the simulation analysis of fixed-step and variable step method of seam tracking control, the correctness and validity to accuracy of analytical methods and modeling presented in this paper were verified, the main reason affecting seam tracking accuracy was seam tracking control algorithm and robot positioning accuracy. The accuracy analysis method have guiding significance for seam tracking control of robot error compensation and the improvement of seam tracking control method.

Key words: seam tracking; robot; accuracy analysis

Diffusion bonding of TiAl to Ni-based superalloy HE Peng[1], LI Haixin[1], LIN Tiesong[1], Huang Yudong[2], LIU Yu[1], QIAN Guotong[3] (1. State Key Laboratory of Advanced Welding and Joining, Harbin institute of Technology, Harbin 150001, China; 2. School of Chemical Engineering and Technonlgy, Harbin institute of Technology, Harbin 150001, China; 3. Shaoxing Tianlong Tin Materials CO., LTD, Shaoxing 312001, China).